Am J Transl Res 2019;11(7):4192-4202
www.ajtr.org /ISSN:1943-8141/AJTR0098280

Original Article

Tumor-derived MDSCs inhibit airway remodeling in asthmatic mice through regulating IL-10 and IL-12

Yanli Zhang[1], Boyi Xu[2], Bin Luan[1], Yan Zhang[1], Xiufang Wang[1], Xiaorong Xiong[1], Hongke Shi[1]

[1]*Department of Pediatrics, The Third Affiliated Hospital of Zhengzhou University, Zhengzhou 450052, China;*
[2]*Institute of Psychology, Chinese Academy of Sciences, Beijing 100101, China*

Received June 10, 2019; Accepted June 29, 2019; Epub July 15, 2019; Published July 30, 2019

Abstract: Myeloid-derived suppressor cells (MDSCs), a group of newly discovered and heterogeneous myeloid-derived immunosuppressive cells, play an important role in the progress of asthma, however, the specific mechanism is still largely unclear. Our previous study has indicated that during the onset of asthma, the accumulation of MDSCs and the level of serum interleukin (IL)-10 increased, while the level of IL-12 decreased. The present study aimed to investigate whether tumor-derived MDSCs could inhibit airway remodeling in asthmatic mice through regulating IL-10 and IL-12 secretion. To perform our investigation, we established a mouse model of breast cancer, and the extracted MDSCs from breast caner mouse model were injected into a mouse model of asthma induced by ovalbumin (OVA). Then, asthmatic airway remodeling of mice was analyzed and the levels of IL-10 and IL-12 in the serum and bronchoalveolar lavage fluid (BALF) of mice were detected. In addition, the correlation of MDSCs with the levels of IL-10 and IL-12 in the transplantation group was analyzed. The transplantation of tumor-derived MDSCs into asthmatic mice significantly improved airway remodeling, decreased MDSCs and the expression of IL-10, and significantly increased the expression of IL-12. Besides, we confirmed that IL-10 was positively correlated with MDSCs, while IL-12 was negatively correlated with MDSCs. The results indicated that tumor-derived MDSCs could reduce IL-10 level, increase the level of IL-12, and thus correct the Th1/Th2 imbalance in asthmatic mice. In summary, our results revealed that tumor-derived MDSCs could serve as a potential novel target for asthma therapy.

Keywords: MDSCs, asthma, IL-10, IL-12, Th1/Th2 imbalance

Introduction

Asthma, a Th2-dominant immune disorder [1], is a common chronic inflammatory disease of the airways and a severe health risk for children [2]. Asthma affects approximately 235 million people worldwide [3]. Despite the availability of national and international asthma management guidelines [4], up to 50% of patients with asthma who are aged 4-18 years show symptoms or signs of inadequate control [5]. Poor control not only contributes to high treatment costs but also correlates with more frequent exacerbations and an increased risk of persistent asthma in children [6, 7]. Therefore, there is a need for effective and well-tolerated treatment options for patients who have inadequate control.

House dust mite (HDM)-induced asthma has translational value, which suggests that it may be particularly well suited for *in vivo* studies involving the effects of pharmacological agents on exacerbation-induced expression of major upstream Th2 cytokines [8]. Significant associations of the IL-10 haplotypes with asthma have been reported. A meta-analysis suggested that IL-10 promoter polymorphism is associated with asthma risk [9], and decreased IL-10 level is important in pediatric asthmatic patients with specific genotypes [10]. Ferulic acid could induce Th1 response by modulating the function of dendritic cells and ameliorate Th2-mediated allergic airway inflammation in mice [11]. These studies indicated that IL-10 and IL-12 play important roles in the occurrence and development of asthma.

MDSCs constitute a key checkpoint that impedes tumor immunity against cancer. A study has reported a unique mechanism by which monocytic (M)-MDSCs are spared, allowing

them to polarize towards M1 macrophages for the reactivation of immunity against breast cancers [12]. Tregs and MDSCs are significantly increased in hosts with advanced malignancies. MDSCs mediate the suppression of the tumor antigen-specific T cell response through the induction of T cell anergy and the development of Tregs in tumor-bearing mice [13]. A previous report suggests that MDSCs reduce to normal levels or below normal levels by neoadjuvant chemotherapy alone [14].

Immunosuppressive MDSCs induced by TLR signaling during infection (by various bacteria, parasites and viruses) play a key role in resolution of inflammation [15]. Increased MDSCs can increase IL-10 level and reduce IL-12 level, resulting in an asthma-related Th1/Th2 imbalance [16]. Besides, tumor-derived MDSCs inhibit the Th2 cell-mediated response against allergens in a TGF-β1-dependent manner. Based on these collective results, asthma may be effectively targeted using a novel MDSC-based cell therapy approach [17]. Whether and how tumor-derived MDSCs regulate the immune response in an asthma environment is currently unclear and worth further study. Furthermore, it is worthwhile to investigate different organs to determine which part of a tumor-bearing mouse can yield a higher proportion of MDSCs.

Our previous study has reported that during the onset of asthma, the accumulation of MDSCs and the level of serum IL-10 increased, while the level of IL-12 decreased, indicating the important roles in the development of asthma. However, whether tumor-derived MDSCs could inhibit airway remodeling in asthmatic mice through regulating the expression of IL-10 and IL-12 is currently unclear.

Therefore, the purpose of this study was to reveal the role of tumor-derived MDSCs in asthmatic mice, and to further explore the relationship between MDSCs and the expression of IL-10 and IL-12.

Materials and methods

Ethics statement

All procedures were carried out in accordance with the relevant guidelines and regulations. All experimental protocols were approved by a specially appointed institutional and/or licensing committee. Specifically, for animal studies, all protocols were reviewed and approved by the Animal Ethics Committees of the Third Affiliated Hospital of Zhengzhou University under University Animal Research Guideline 1996-21. The animals were housed and treated under approved protocols, and all efforts were made to minimize animal suffering.

Animal studies

Sixty specific pathogen-free (SPF)-grade 6- to 8-week-old female BALB/c mice (body weight: 20 ± 2 g) were provided by Zhengzhou University Animal Experiment Center (serial number: SCXK [Yu] 2015-0006). The animals were housed in the Experiment Center of the Third Affiliated Hospital of Zhengzhou University with free access to food and water for one week prior to the initiation of the experiment. The mice were divided into four groups: saline control (Control), ovalbumin (OVA)-induced asthmatic mice (Asthma), asthmatic mice treated with budesonide (Intervention), and asthmatic mice treated with tumor-derived MDSCs (Transplation).

The asthmatic mouse model was established based on a previous study, with some modifications [18]. Briefly, each mouse was injected intraperitoneally with 0.2 ml of OVA (Sigma-Aldrich, St. Louis, MO, USA)/aluminum hydroxide on day 1, 8, and 15 and then stimulated with 2% OVA inhalation for 30 min every other day, starting from day 22, for a total of 10 doses. Asthma was established in the treatment groups using the same procedure, except for an additional 30 min of inhalation treatment with 1 mg (2 ml) of budesonide (Intervention). For the transplantation group, during the third week of induction, the MDSCs were firstly adjusted to 1×10^7 cells/ml, and 0.2 ml of the suspension was injected into mouse through the vein once per day, for a total of 7 injections. Saline was used for the control group, and the method and dose were the same as those used for the asthma group. All mice survived during the experiment.

Evaluation of the OVA-induced murine asthma model

The mice were divided into asthma group and control group. No statistically significant differences between these two groups in terms of body weight, activity level, or reaction to stimuli were detected prior to the experiment. No swell-

ing or ulcers were observed during or after intraperitoneal injection. Three days after the stimulation, the mice in the asthma group displayed restlessness, sneezing, and deepened breathing, which stopped approximately 10 min after completing the 30-min OVA stimulation. Five days after the OVA stimulation, the mice in the asthma group displayed either hypomania or a significant reduction in activity levels. The mice in the control group behaved as they did before the experiment, exhibiting healthy appetites, agile movement, and glossy fur. Mice that displayed shortened breath, restlessness, cyanosis, salivation, and fecal and urine incontinence after inhalation of the allergen indicated successful establishment of the asthmatic mouse model. More severe reactions included hypopnea or respiratory arrhythmia, respiratory failure, and lethargy. All mice were evaluated by H&E staining, IHC, and PAS staining for asthmatic markers, such as inflammatory cells and thickening of the airway smooth muscles, airway walls, and epithelial mucosa.

Isolation of serum from mice

Mouse blood was collected by sterile retroorbital bleeding, allowed to clot at room temperature, and centrifuged for 10 min at 2000 rpm. Serum was collected from the top layer in the tube and aliquoted for use in experiments.

Enzyme linked immunosorbent assay (ELISA)

The levels of IL-10 and IL-12 in the serum of mice form different groups were determined using IL-10 and IL-12 ELISA Detection Kits (R&D Systems, Minneapolis, MN, USA) according to the manufacturer's instructions.

Staining procedures

Staining procedures were performed according to the kit manufacturer's instructions. For H&E staining to detect inflammatory cells, the number of eosinophils, neutrophils, and lymphocytes was averaged from five different areas per slide following microscopic evaluation at a 400 × magnification. IHC was scored by the same researcher on the same microscope. The lung tissues of mice were stained with antibodies specific for MDSCs, and yellow/brown staining was considered to indicate a positive signal. Images were obtained at a 200 × magnification, five positive areas per slice were selected for analysis, and optical density values were measured. The intensity of H&E staining, IHC, and PAS staining were evaluated semiquantitatively using the following categories: 0 (no staining), 1 + (weak but detectable staining), 2 + (moderate or distinct staining), and 3 + (intense staining). For each specimen, a HSCORE value was derived by calculating the sum of the percentages of cells that were stained in each intensity category and multiplying that value by the weighted intensity of staining, using the formula HSCORE = Pi (i + 1), where i represents the intensity score, and Pi is the corresponding percentage of cells. For each slide, five different areas and 100 cells per area were evaluated microscopically with a 40 × objective. The percentage of cells at each intensity within these areas was determined at different times by two investigators who were blinded to the source of the samples, and the average of their scores was used.

BALF cell collection

The mice were anesthetized and stabilized on a wooden board 24 h after the last stimulation, and their chests were opened for the following procedures. The distal trachea and left main bronchus were ligated, each mouse was tracheally intubated with a modified 22-G catheter, and lavage was performed three times with 0.5 ml of cold phosphate-buffered saline (PBS). The BALF was collected with a recycle rate of >85%. The supernatants were collected after 10 min of centrifugation at 4°C and 1500 rpm and stored at -20°C for use in following experiments.

Preparation of a mouse model of breast cancer and extraction of monocyte suspensions from the bone marrow and spleen

Breast cancer cells (4T1) during the growth period were adjusted to a density of 1×10^7 cells/ml with 1 × PBS, and then 0.2 ml of the cell suspension was injected into the right subcutaneous axillary region of the mice. After 10-14 days (the diameter of the tumor increased to 2-4 cm), the mice were sacrificed, soaked in 75% alcohol for 10 min, and washed three times in PBS.

The spleens were ground with a sterile grinding bar, and mononuclear cells were filtered and collected in a 300 mesh sieve. The red blood cells were then lysed, and the samples were washed two times in PBS. A Gr-1 monoclonal

antibody (McAb) (FACSCalibur, BD Biosciences) conjugated to fluorescein isothiocyanate (FITC) (FACSCalibur, BD Biosciences) and a CD11b McAb conjugated to phycoerythrin (PE) (FACSCalibur, BD Biosciences) were incubated with the samples at 4°C in the dark for 20 min. Then, the McAbs were washed twice with PBS, and the proteins were detected by flow cytometry (FCM). In addition, the tibias and femurs of the mice were separated, and 1 ml of PBS in a 5 ml syringe was used to rinse the marrow cavity 2-3 times. The rinses were collected, filtered through a 300 mesh strainer, and centrifuged at 1000 rpm for 10 min. The clear liquid was discarded, and red blood cell lysis buffer was added. The samples were vortexed and allowed to stand for 5 min before centrifugation and storage until use.

Flow cytometry cell separation: The McAbs (an anti-Gr-1 antibody conjugated to FITC and an anti-CD11b antibody conjugated to PE) were incubated with the samples at 4°C in the dark for 30 min, and the samples were washed 2 times with PBS and subjected to FCM to sort CD11b and Gr-1 double-positive cells.

MDSCs selection and purification by immunomagnetic beads: Magnetic beads conjugated to antibodies specific for CD11b and Gr-1 were added to the selected cell suspensions at a density of 10^7 cells/90 μl; the density was adjusted to 10^7 cells/10 μl, and the suspensions were incubated at 4°C in the dark for 15 min. First, the magnetic bead separation columns were equilibrated. Then, 500 μl of buffer was added; after the buffer flowed through, the same amount of buffer was added again, for a total of 3 times. Finally, 1 ml of buffer was added, the separation column was removed, and CD11b and Gr-1 double-positive cells were obtained.

Proportions of MDSCs in single-cell suspensions of spleen and bone marrow: Fluorescence-labeled antibodies (anti-Gr-1-PE and anti-CD11b-FITC) were added to the cell suspension, which was prepared for detection. Then, the suspension was incubated at 4°C for 15 min and subsequently tested by a flow cytometer.

Statistical analysis

All data were analyzed with SPSS 21.0 software (IBM, Chicago, IL, USA) and presented as the mean ± standard deviation (SD). Each set of data was determined to conform to a normal distribution, analyzed by the F-test for homogeneity of variance, and then subjected to univariate analysis between groups in a multiapplication, pairwise comparison with the Bonferroni correction; t-tests were used for comparisons between two groups. Correlations were determined by the Pearson correlation, with $P<0.05$ set as the criterion for statistical significance.

Results

4T1 cell microscopic findings and tumors in mice with breast cancer

To explore the role of MDSCs induced by tumor cells in asthmatic mice and its relationship with IL-10 and IL-12, breast cancer tumor was established in a mouse model. MDSCs were marked, extracted, and injected into an asthmatic mouse model.

Breast cancer cells during the growth period were was adjusted to a density of 1×10^7 cells/ml with 1 × PBS, and 0.2 ml of the cell suspension was injected into the right subcutaneous axillary region of the mice after 10-14 days. 4T1 cells with a single layer of wall growth. Twenty-four hours after inoculation, the morphology of 4T1 breast cancer cells under an electron microscope (20 ×) (**Figure 1A**). After approximately 3-4 days, the cells reached 80% confluence, and the cells were in logarithmic growth. The cells were then collected for injection into mice, and **Figure 1B** presented the tumor-bearing mouse.

Comparison of the spleen between control mice and tumor-bearing mice

We compared spleen morphologies and weights between control mice and tumor-bearing mice. A comparison of the spleen morphologies was shown in **Figure 2A**, and the spleen weights were shown in **Figure 2B**. The spleen weight of the control mice (0.13 ± 0.06 g) was much lower than that of the tumor-bearing mice (0.47 ± 0.13 g).

Comparison of the proportion of MDSCs extracted from the spleen and bone marrow of tumor-bearing mice, as detected by FCM

We applied FCM to detect the proportions of MDSCs derived from the spleen and bone mar-

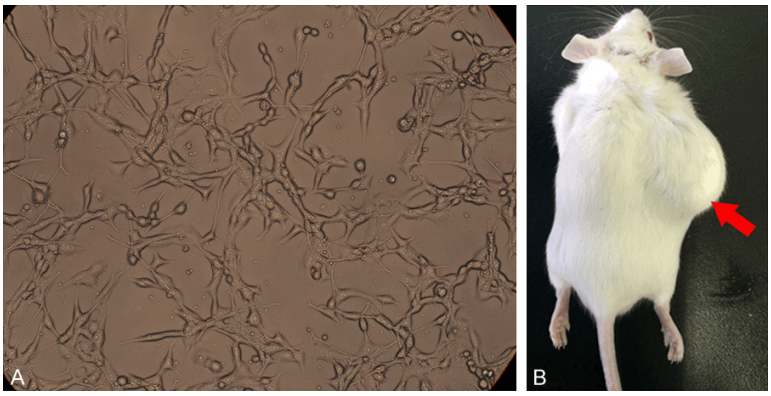

Figure 1. 4T1 cell microscopic findings related to breast cancer cells and tumors in mice with breast cancer. A: The morphology of 4T1 breast cancer cells under an electron microscope (20 ×), the cells under the inverted microscope showed a single layer of adherent growth. B: Breast cancer-bearing mice.

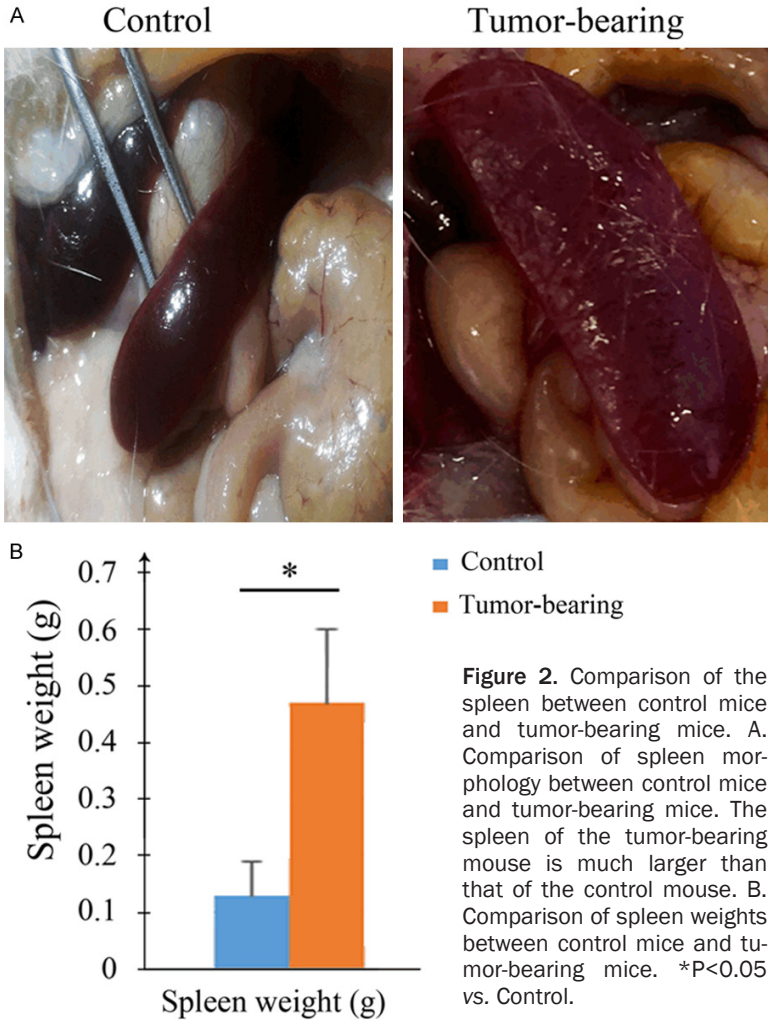

Figure 2. Comparison of the spleen between control mice and tumor-bearing mice. A. Comparison of spleen morphology between control mice and tumor-bearing mice. The spleen of the tumor-bearing mouse is much larger than that of the control mouse. B. Comparison of spleen weights between control mice and tumor-bearing mice. *P<0.05 *vs.* Control.

row (**Figure 3A**). The proportion of MDSCs in the spleen suspension (56.20 ± 8.20%) was much lower that in the bone marrow cell suspension (86.30 ± 10.60%) (**Figure 3B**). The data indicated that the proportion of MDSCs extracted from spleen is much lower than that extracted from the bone marrow in tumor-bearing mice.

Comparison of H&E and PAS staining of lung tissues from the mice in each group

We first confirmed that the asthmatic mouse model was established by analyzing the pathological changes in control mice, asthmatic mice, and budesonide-treated mice. H&E staining of lung tissues from the asthmatic mice exhibited submucosal edema, mucous gland hyperplasia, and increased mucous secretion, accompanied by increased mucosal folds, visible epithelial fractures, epithelial cell shedding, mild bronchiole smooth muscle hypertrophy, and bronchial wall and basement membrane thickening and shape irregularities (**Figure 4A** and **4B**).

Each group had different pathological changes. The airway remodeling in the asthma group was significantly greater than that in the control group. The airway remodeling changes in the intervention group and the transplantation group were significantly alleviated compared to those in the asthma group (**Figure 4A**), as demonstrated by H&E staining and PAS staining. The thickness of the airway smooth muscle (μm), airway wall (μm) and epithelial mucosa (μm) was determined by H&E staining of tissues from mice in the control group, the asthma group, and the groups of asthmatic mice treated with budesonide or MDSCs from

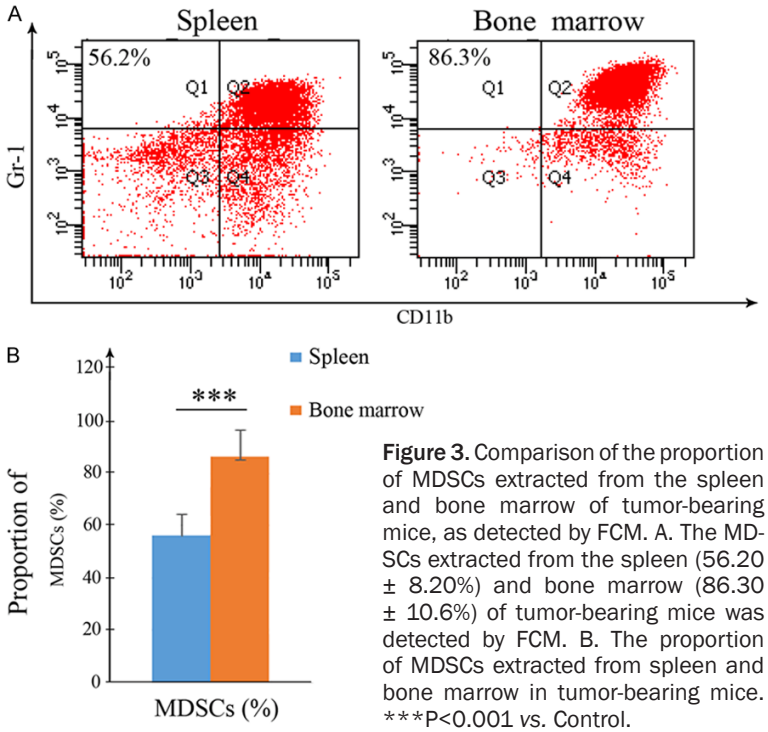

Figure 3. Comparison of the proportion of MDSCs extracted from the spleen and bone marrow of tumor-bearing mice, as detected by FCM. A. The MDSCs extracted from the spleen (56.20 ± 8.20%) and bone marrow (86.30 ± 10.6%) of tumor-bearing mice was detected by FCM. B. The proportion of MDSCs extracted from spleen and bone marrow in tumor-bearing mice. ***P<0.001 *vs.* Control.

breast tumor-bearing mice (**Figure 4B**). The asthmatic mice exhibited significantly higher levels of pathological changes than the mice in the control group and the treatment groups. These results indicated that the asthma model was established and that the intervention and transplantation therapies were effective.

Comparison of the levels of IL-10 and IL-12 in the BALF and serum of the mice in each group

We then explored the effect of MDSCs induced by tumor cells on the expression of Il-10 and Il-22 in asthmatic mice. The IL-10 and IL-12 levels of BALF (**Figure 5A**) and serum (**Figure 5B**) in mice of each group were detected by ELISA, and results indicated that the level of IL-10 in the asthma group was significantly higher than that in the control group, while the level of IL-12 was significantly decreased. Compared with the asthma group, the levels of IL-10 in the BALF (**Figure 5A**) and serum (**Figure 5B**) of asthmatic mouse significantly reduced in the intervention and transplation groups, while the levels of IL-22 significantly enhanced.

Comparison of MDSCs in lung tissues from the mice in each group

To observe the changes of MDSCs in the asthma group, the control group, the intervention group and the transplation, the MDSCs levels of each group were measured by immunohistochemical staining and FCM. Quantification of IHC (HSCORE) of MDSCs from mice in each group was performed.

We found that the number of MDSCs in the asthma group was significantly higher than that in the control group. The number of MDSCs in the intervention group and the transplantation group was significantly lower than that in the control group (**Figure 6A** and **6C**). A comparison of the MDSCs extracted by FCM in each group yielded similar results to those obtained via immunohistochemical staining (**Figure 6B** and **6D**).

Correlation analysis of MDSCs with the expression of IL-10 and IL-12 in the transplantation group

Finally, we analyzed the relationship between MDSCs and the expression of IL-10 and IL-12 in asthmatic mice. We performed IHC of MDSCs in tissues from asthmatic mice treated with MDSCs from breast tumor-bearing mice, and IHC of MDSCs was quantified (HSCORE).

The serum IL-10 and IL-12 levels of mice from the transplantation group were detected by ELISA, and the correlations between MDSCs and IL-10 and IL-12 expression in the transplantation group were analyzed. Results indicated that MDSCs was positively correlated with serum IL-10 level (**Figure 7A**) and negatively with serum IL-12 level (**Figure 7B**) in asthmatic mice.

Discussion

MDSCs have different functions in different conditions. Isolated and purified MDSCs have been found to play a therapeutic role in autoimmune diseases and transplantation immunity. There are few reports on the negative immunoregulation effect of MDSCs in asthma. Bone marrow is the main gathering place of MDSCs under normal physiological conditions, and

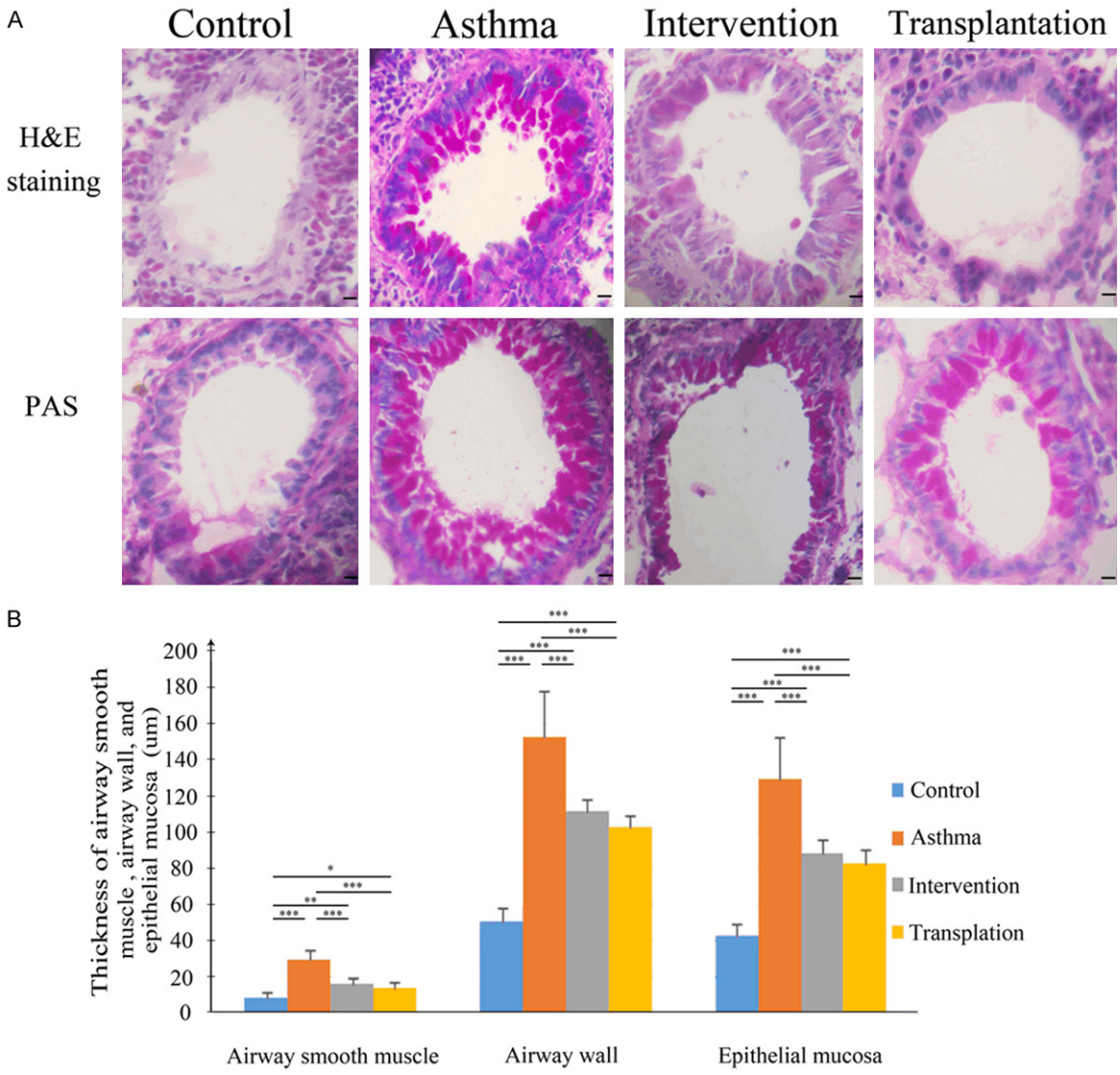

Figure 4. Comparison of H&E and PAS staining of lung tissues from the mice in each group. Pathological changes in the lung tissues of asthmatic mice and asthmatic mice treated with budenoside or MDSCs from breast tumor-bearing mice. A. H&E staining (upper) and PAS staining (lower) of mouse lung tissues respectively from the control group, the asthma group, and the groups of asthmatic mice treated with budenoside or MDSCs from breast tumor-bearing mice. All images were obtained at a 200 × magnification. The scale bar represented 80 μm. B. The thickness of the airway smooth muscle (μm), airway wall (μm) and epithelial mucosa (μm) were determined by H&E staining of tissues from mice in the control group, the asthma group, and the groups of asthmatic mice treated with budesonide or MDSCs from breast tumor-bearing mice. All data were presented as the mean ± SD. *P<0.05, **P<0.01, and ***P<0.001.

these cells can differentiate into mature macrophages and dendritic cells [18]. MDSCs increase significantly in tumors, during inflammation, and in other diseases and exert a negative immunomodulatory effect [19]. The use of bio-markers for immune surveillance can be applied to the clinical classification and follow-up of patients and provide new predictive and diagnostic tools for clinical practice. MDSCs can be used as a new target for chronic inflammatory conditions, such as bronchial asthma [20].

Different sub-types of MDSCs have different functions, and MDSCs have an immunosuppressive function in cancer [18]. MDSCs are a heterogeneous population of cells that consist of myeloid progenitor cells and immature myeloid cells. MDSCs have been identified as a cell population that may affect CD4(+) and

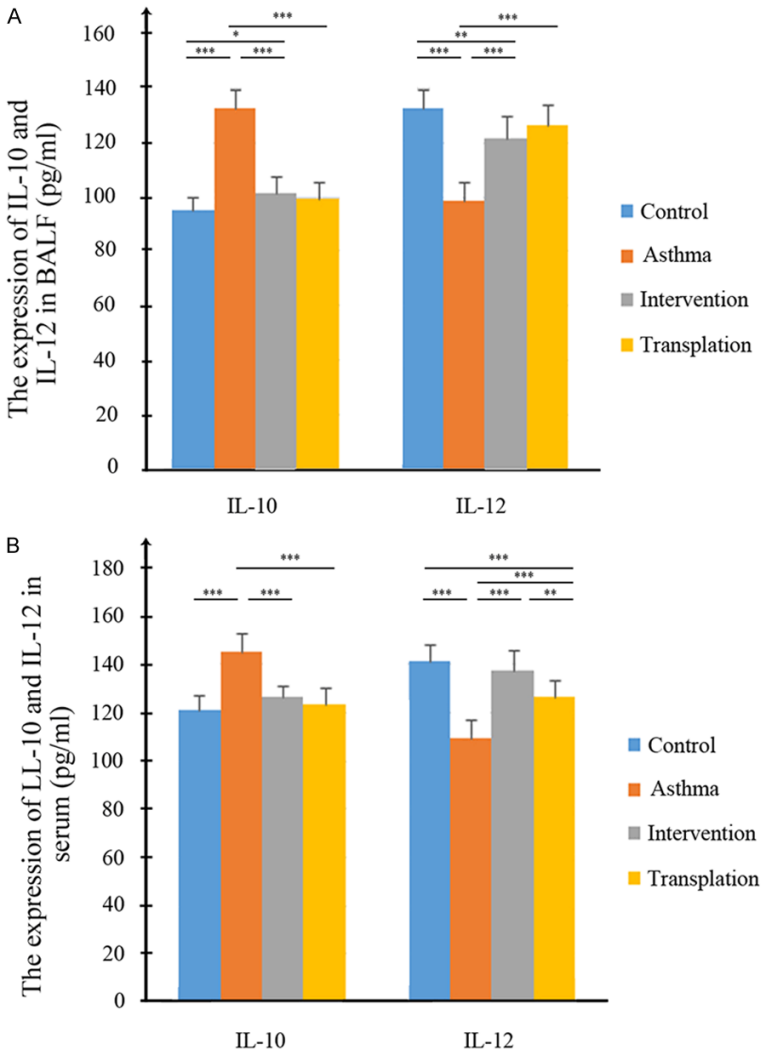

Figure 5. Comparison of the levels of IL-10 and IL-12 in the BALF and serum of the mice in each group. Levels of asthma-related cytokines (IL-10 and IL-12) in mouse BALF (A) and serum (B) were determined by ELISA. All data were presented as the mean ± SD. *P<0.05, **P<0.01, and ***P<0.001.

CD8(+) T cell activation to negatively regulate immune responses, making these cells an attractive target for the treatment of transplant patients and autoimmune disease patients. The roles of MDSCs in different transplantation and autoimmune disease models and the potential to target these cells for therapeutic benefit have been investigated [21]. However, there are few studies on the negative immunoregulation effects of MDSCs in asthma. Studies have reported that MDSCs can be isolated from the spleen or peripheral blood of tumor-bearing mice or mice with severe infections [22]. However, how to extract MDSCs more effectively has not been investigated.

The 4T1 breast cancer mice used in this study were generated from 6- to 8-week-old BALB/c mice. The spleens of the tumor-bearing mice were significantly heavier than those of the control mice. The breast cancer cells were polymorphous, and desmosomes were seen at the junctions of the cells. Mucin particles and cell bodies were seen in the cytoplasm, suggesting that predominantly the breast cancer cell grew and that the mouse model of breast cancer was successfully established. In addition, MDSCs could be extracted from the spleen and bone marrow of the mice. The proportion of MDSCs extracted from the bone marrow cell suspension was higher than that extracted from the spleen, suggesting that high-purity MDSCs could be isolated from the bone marrow cell suspension of tumor-bearing mice. This finding laid a foundation for studying the inhibition of airway inflammatory responses after the transplantation of exogenous MDSCs into asthmatic mice.

MDSCs from different sources play roles in immunosuppression through different pathways in different micro-environments. In tumor-bearing animals, MDSCs inhibit CD4(+) and CD8(+) T cells, B cells and natural killer (NK) cells [23], probably by promoting the secretion of nitric oxide (NO), arginine depletion, and the production of oxygen free radicals and TGF-β [24]. In tumor-bearing mice, the development of immune tolerance is the result of MDSC-induced high expression of Treg Foxp3 [25]. MDSCs can negatively regulate asthma, and the mechanism may due to the role of MDSCs in inhibiting T cells. This function is achieved via increased iNOS levels after the up-regulation of arginase I, which leads to the release of more NO and ROS [26, 19]; the other regulatory pathway is the down-

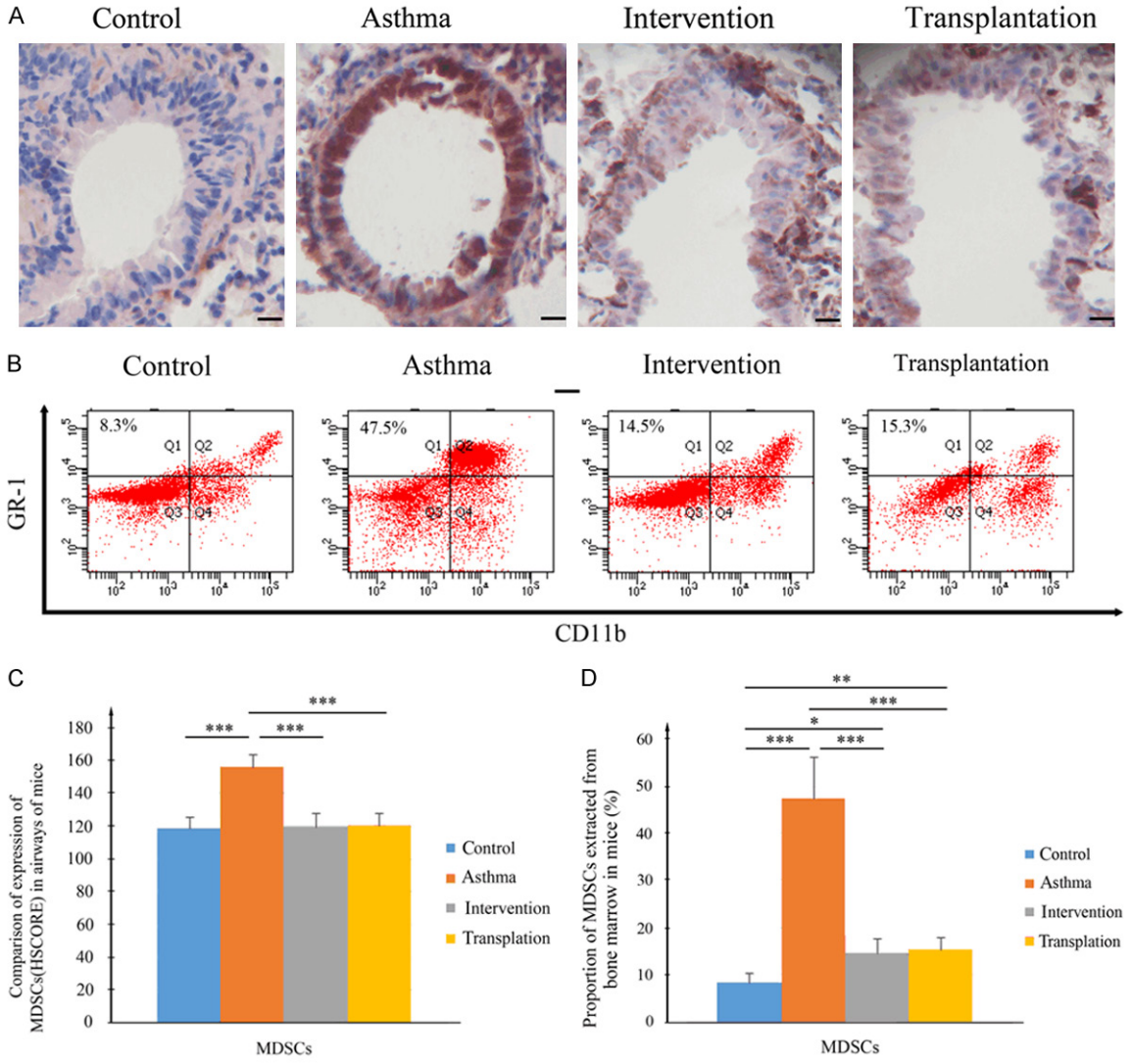

Figure 6. Comparison of MDSCs in lung tissues from the mice in each group. MDSCs in the lung tissues of OVA-induced asthmatic mice, asthmatic mice treated with budenoside or MDSCs from breast tumor-bearing mice and control mice. A. MDSCs in the lung tissues from mice in each group obtained via immunohistochemical staining. All images were obtained at a 200 × magnification. The scale bar represented 80 μm. B. MDSCs extracted by FCM from mice in the control group, the OVA-induced asthma group, and OVA-induced asthmatic mice that were treated with budenoside or MDSCs from breast tumor-bearing mice. C. Analysis statistics of MDSCs in the airways of mice in each group. D. Analysis statistics of MDSCs in the bone marrow of mice in each group. All data were presented as the mean ± SD. *P<0.05, **P<0.01, and ***P<0.001.

regulation of L-selectin on the surface of T cells, which is a result of MDSC inhibition [27]. The Th2 cell-mediated inflammatory response is the result of exogenous MDSCs, which inhibit the expression of TGF-β1 that is induced by the allergen [17].

The labeled MDSCs extracted after LPS stimulation can inhibit airway inflammation and ultimately improve airway inflammation by reversing the proportion of Th1/Th2 cells, increasing the proportion of Tregs and decreasing IL-4 [28]. The immunosuppressive activity of CD11b (+) Gr-1 (+) Ly6G (+) Ly6C (int) MDSCs is weakened in allergen-induced COX-1 gene knockout asthma mice and asthmatic patients with aspirin intolerance, which may be achieved through an EP4-mediated signal transduction pathway [29]. Thus, we envisaged that MDSCs may be used as a new method for treating asthma.

This study investigated whether MDSCs played a negative immunomodulatory role during asthma. The results demonstrated that airway inflammation and airway remodeling were most

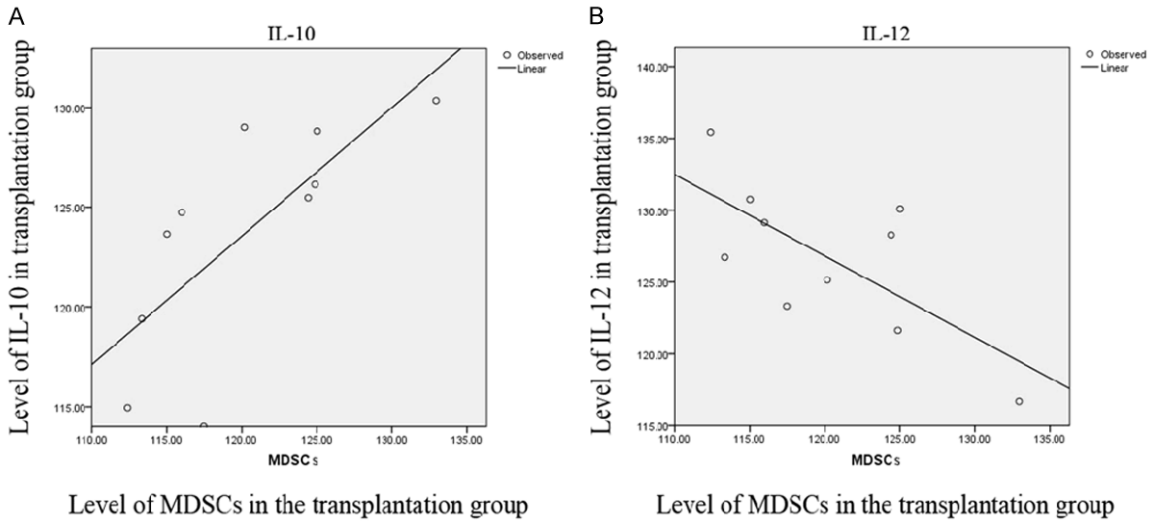

Figure 7. Correlation analysis of MDSCs with the expression of IL-10 and IL-12 in the transplantation group. Correlation between the quantification of IHC (HSCORE) of MDSCs in mice treated with MDSCs from breast tumor-bearing mice and the restoration of the Th1/Th2 balance in mice from the transplantation group experiencing asthma relief. A. Positive correlation between the quantification of IHC (HSCORE) of MDSCs and serum levels of IL-10 were determined by ELISA Correlation analysis was performed to assess the animal correlation; $r = 0.538$ and $P<0.05$. B. Negative correlation between the quantification of IHC (HSCORE) of MDSCs and the serum levels of IL-12 was determined by ELISA. Correlation analysis was performed to assess the animal correlation; $r = -0.491$ and $P<0.05$.

obvious in asthmatic mice, and the transplantation group and the intervention group exhibited significant asthma relief. Transplantation of MDSCs isolated from a mouse model of breast cancer could inhibit the airway remodeling of asthmatic mice. The enhanced IL-10 level and of decreased IL-12 level in asthmatic mice were inhibited by MDSCs transplantation. These findings suggested that MDSCs isolated from breast cancer mouse model might be able to inhibit asthmatic airway remodeling by regulating the Th1/Th2 imbalance via altering the levels of IL-10 and IL-12. MDSCs extracted from tumor-bearing mice could be used as a new target for asthma treatment, especially for patients with poor hormone effects or concerns about the use of hormones. To determine the exact mechanism by which exogenous MDSCs inhibited asthma and investigate the application of these cells during later periods, further in-depth study is needed.

Acknowledgements

The present study was supported by the Henan Province Medical Science and Technology Breakthrough Plan Project (No. 201503114).

Disclosure of conflict of interest

None.

Address correspondence to: Boyi Xu, Institute of Psychology, Chinese Academy of Sciences, No. 16 Zhongzhi Road, Chaoyang District, Beijing 100101, China. Tel: 010-64888628; Fax: 010-64888628; E-mail: xuboyi110619@163.com

References

[1] Robinson DS, Hamid Q, Ying S, Tsicopoulos A, Barkans J, Bentley AM, Corrigan C, Durham SR and Kay AB. Predominant TH2-like bronchoalveolar T-lymphocyte population in atopic asthma. N Engl J Med 1992; 326: 298-304.

[2] Herrera AM, Fitzgerald DA. Question 1: why do children still die from asthma? Paediatr Respir Rev 2018; 27: 40-43.

[3] Organization WH. Asthma. 2011. Fact Sheet 2017.

[4] Asthma Glf. 2017 GINA report, global strategy for asthma management and prevention. 2017.

[5] Schmier JK, Manjunath R, Halpern MT, Jones ML, Thompson K and Diette GB. The impact of inadequately controlled asthma in urban children on quality of life and productivity. Ann Allergy Asthma Immunol 2007; 98: 245-51.

[6] Belgrave DC, Buchan I, Bishop C, Lowe L, Simpson A and Custovic A. Trajectories of lung function during childhood. Am J Respir Crit Care Med 2014; 189: 1101-1109.

[7] Custovic A, Johnston SL, Pavord I, Gaga M, Fabbri L, Bel EH, Le Souëf P, Lötvall J, Demoly P, Akdis CA, Ryan D, Mäkelä MJ, Martinez F,

Holloway JW, Saglani S, O'Byrne P, Papi A, Sergejeva S, Magnan A, Del Giacco S, Kalayci O, Hamelmann E, Papadopoulos NG. EAACI position statement on asthma exacerbations and severe asthma. Allergy 2013; 68: 1520-1531.

[8] Persson IM, Akbarshahi H, Menzel M, Brandelius A and Uller L. Increased expression of upstream TH 2-cytokines in a mouse model of viral-induced asthma exacerbation. J Transl Med 2016; 14: 52.

[9] Nie W, Fang Z, Li B and Xiu QY. Interleukin-10 promoter polymorphisms and asthma risk: a meta-analysis. Cytokine 2012; 60: 849-855.

[10] Kerley C, Hutchinson K, Faul J, Greally P, Coghlan D, Elnazir B, Louw M and Rochev Y. Vitamin D receptor variants and uncontrolled asthma. Eur Ann Allergy Clin Immunol 2018; 50: 108-116.

[11] Lee CC, Wang CC, Huang HM, Lin CL, Leu SJ and Lee YL. Ferulic acid induces Th1 responses by modulating the function of dendritic cells and ameliorates Th2-mediated allergic airway inflammation in mice. Evid Based Complement Alternat Med 2015; 2015: 678487.

[12] Ugel S, Delpozzo F, Desantis G, Papalini F, Simonato F, Sonda N, Zilio S and Bronte V. Therapeutic targeting of myeloid-derived suppressor cells. Curr Opin Pharmacol 2009; 9: 470-481.

[13] Kao J, Ko EC, Eisenstein S, Sikora AG, Fu S and Chen SH. Targeting immune suppressing myeloid-derived suppressor cells in oncology. Crit Rev Oncol Hematol 2011; 77: 12-9.

[14] Verma C, Eremin JM, Robins A, Bennett AJ, Cowley GP, El-Sheemy MA, Jibril JA and Eremin O. Abnormal T regulatory cells (Tregs: FOXP3+, CTLA-4+), myeloid-derived suppressor cells (MDSCs: monocytic, granulocytic) and polarised T helper cell profiles (Th1, Th2, Th17) in women with large and locally advanced breast cancers undergoing neoadjuvant chemotherapy (NAC) and surgery: failure of abolition of abnormal treg profile with treatment and correlation of treg levels with pathological response to NAC. J Transl Med 2013; 11: 16.

[15] Ray A, Chakraborty K and Ray P. Immunosuppressive MDSCs induced by TLR signaling during infection and role in resolution of inflammation. Front Cell Infect Microbiol 2013; 3: 52.

[16] Zhang YL, Luan B, Wang XF, Qiao JY, Song L, Lei RR, Gao WX and Liu Y. Peripheral blood MDSCs, IL-10 and IL-12 in children with asthma and their importance in asthma development. PLoS One 2013; 8: e63775.

[17] Song C, Yuan Y, Wang XM, Li D, Zhang GM, Huang B and Feng ZH. Passive transfer of tumour-derived MDSC s inhibits asthma-related airway inflammation. Scand J Immunol 2014; 79: 98-104.

[18] Qu P, Wang LZ and Lin PC. Expansion and functions of myeloid-derived suppressor cells in the tumor microenvironment. Cancer Lett 2016; 380: 253-6.

[19] Nagaraj S, Youn JI and Gabrilovich DI. Reciprocal relationship between myeloid-derived suppressor cells and T cells. J Immunol 2013; 191: 17-23.

[20] Rudensky AY. Regulatory T cells and Foxp3. Immunol Rev 2011; 241: 260-8.

[21] Zhang Q, Fujino M, Xu J and Li XK. The role and potential therapeutic application of myeloid-derived suppressor cells in allo-and autoimmunity. Mediators Inflamm 2015; 2015: 421927.

[22] Cuenca AG, Delano MJ, Kelly-Scumpia KM, Moreno C, Scumpia PO, LaFace DM, Heyworth PG, Efron PA and Moldawer LL. A paradoxical role for myeloid-derived suppressor cells in sepsis and trauma. Mol Med 2011; 17: 281-92.

[23] Lindau D, Gielen P, Kroesen M, Wesseling P and Adema GJ. The immunosuppressive tumour network: myeloid-derived suppressor cells, regulatory T cells and natural killer T cells. Immunology 2013; 138: 105-115.

[24] Raber P, Ochoa AC and Rodríguez PC. Metabolism of L-arginine by myeloid-derived suppressor cells in cancer: mechanisms of T cell suppression and therapeutic perspectives. Immunol Invest 2012; 41: 614-34.

[25] Hoechst B, Ormandy LA, Ballmaier M, Lehner F, Krüger C, Manns MP, Greten TF and Korangy F. A new population of myeloid-derived suppressor cells in hepatocellular carcinoma patients induces CD4+ CD25+ Foxp3+ T cells. Gastroenterology 2008; 135: 234-243.

[26] Forster R, Davalos-Misslitz AC and Rot A. CCR7 and its ligands: balancing immunity and tolerance. Nat Rev Immunol 2008; 8: 362-71.

[27] Sun LG, Guo JF, Brown R, Amagai T, Zhao Y and Su DM. Declining expression of a single epithelial cell-autonomous gene accelerates age-related thymic involution. Aging Cell 2010; 9: 347-357.

[28] Fan HZ, Yu HP, Yu R, Zhang Y, Deng HJ and Chen X. Passive transfer of lipopolysaccharide-derived myeloid-derived suppressor cells inhibits asthma-related airway inflammation. Eur Rev Med Pharmacol Sci 2015; 19: 4171-81.

[29] Shi MH, Shi GC, Tang J, Kong DP, Bao Y, Xiao B, Zuo CJ, Wang T, Wang QS, Shen YJ, Wang H, Funk CD, Zhou J and Yu Y. Myeloid-derived suppressor cell function is diminished in aspirin-triggered allergic airway hyperresponsiveness in mice. J Allergy Clin Immunol 2014; 134: 1163-1174.